Competing droughts affect dust delivery to Sierra Nevada

Aarons, S. M.; Arvin, L. J.; Aciego, S. M.; Riebe, C. S.; Johnson, K. R.; Blakowski, M. A.; Koornneef, J. M.; Hart, S. C.; Barnes, M. E.; Dove, N.; Botthoff, J. K.; Maltz, M.; Aronson, E. L.

published in
Aeolian Research
2019

DOI (link to publisher)
10.1016/j.aeolia.2019.100545

document version
Publisher's PDF, also known as Version of record

Aeolian Research 41 (2019) 100545

Contents lists available at ScienceDirect

Aeolian Research

journal homepage: www.elsevier.com/locate/aeolia

Invited Research article

Competing droughts affect dust delivery to Sierra Nevada

S.M. Aarons[a,b,*], L.J. Arvin[c], S.M. Aciego[c], C.S. Riebe[c], K.R. Johnson[d], M.A. Blakowski[e], J.M Koornneef[f], S.C. Hart[g], M.E. Barnes[g], N. Dove[g], J.K. Botthoff[h], M. Maltz[g,h], E.L. Aronson[i]

[a] Scripps Institution of Oceanography, University of California San Diego, San Diego, CA 92037, USA
[b] Department of Geophysical Sciences, University of Chicago, Chicago, IL 60637, USA
[c] Department of Geology and Geophysics, University of Wyoming, Laramie, WY 82071, USA
[d] Department of Earth System Sciences, University of California, Irvine, CA 92697, USA
[e] Department of Earth and Environmental Sciences, University of Michigan, Ann Arbor, MI 48109, USA
[f] Faculty of Earth and Life Sciences, Vrije Universiteit Amsterdam, 1081HV Amsterdam, the Netherlands
[g] Department of Life & Environmental Sciences and the Sierra Nevada Research Institute, University of California, Merced, CA 95343, USA
[h] Center for Conservation Biology, University of California, Riverside, CA 92521, USA
[i] Department of Microbiology and Plant Pathology, University of California, Riverside, CA 92521, USA

ARTICLE INFO

Keywords:
Biogeochemistry
Drought
Dust supply
Mineral dust
Nutrient delivery

ABSTRACT

The generation and transport of mineral dust is strongly related to climate on seasonal, year-to-year, and glacial-interglacial timescales. The modern dust cycle is influenced by soil moisture, which is partly a function of drought duration and severity. The production and transport of dust can therefore be amplified by global and regional droughts, thereby moderating ecosystem vulnerability to disturbance through the influence of dust on nutrient delivery to ecosystems. In this work, we use strontium and neodymium isotopes in combination with trace element concentrations in modern dust samples collected in 2015 to quantify the role of regionally versus globally supplied dust in nutrient delivery to a montane ecosystem. The study sites lie along an elevational transect in the southern Sierra Nevada, USA, with samples spanning the dry seasons of 2014 (Aciego et al., 2017) and 2015 (this study), when the region was experiencing a historic drought. The goal of our research was to quantify the spatial and temporal variability and sensitivity of the dust cycle to short term changes at nutrient-limited sites. We find that, during the dry season of 2015, Asian sources contributed between 10 and 40% of dust to sites located along this elevational transect, and importantly increased in importance during the summer growing season compared to regional dust sources. These changes are likely related to the prolonged drought in Asia in 2015, highlighting both the sensitivity of dust production and transport to drought and the teleconnections of dust transport in terrestrial ecosystems.

1. Introduction

The mineral dust cycle is sensitive to changes in Earth's climate. Geologic records indicate that the mineral dust flux during glacial periods was one-to-two orders of magnitude higher compared to interglacial periods (Kohfeld and Harrison, 2001). The global dust flux can change on shorter timescales as well, with recent evidence pointing to large fluctuations throughout the last 50 years (Aarons et al., 2016; Evan et al., 2016; Mahowald et al., 2010; Shao et al., 2013). One important challenge facing modern society is understanding how the dust cycle will respond to a changing climate. Increased greenhouse gas forcing and subsequent rises in global temperatures strongly affect moisture supply and potential evapotranspiration (Cook et al., 2014), which are key drivers of droughts. Changes in the frequency, duration, and severity of droughts as a function of climate change will impact human populations by decreasing water resources and disrupting agricultural productivity (Li et al., 2011). Global circulation model (GCM) simulations projecting climate trends into the 21st century indicate that mid-latitude areas in the Northern Hemisphere will experience intensified potential evapotranspiration, which will result in heightened drought risk (Cook et al., 2014), and the Southwest of western North America is expected to experience increased drought severity in the coming decades (Cook et al., 2015). One way to probe the accuracy of GCM model predictions of future mid-latitude drying is to identify changes in aridity reflected in the geochemistry of terrestrial environments. One by-product of heightened drought conditions is the generation and transport of mineral dust, which can be intensified by land use change (Mahowald et al., 2010; Prospero and Lamb, 2003).

* Corresponding author at: Scripps Institution of Oceanography, University of California San Diego, San Diego, CA 92037, USA.
E-mail address: saarons@ucsd.edu (S.M. Aarons).

https://doi.org/10.1016/j.aeolia.2019.100545
Received 1 February 2019; Received in revised form 10 September 2019; Accepted 10 September 2019
Available online 18 September 2019
1875-9637/

Human-induced land use changes, such as agriculture, animal grazing, and heightened industrial activities, have resulted in increased regional dust emissions in the western United States (Neff et al., 2008); dust emissions in some regions have increased by up to 400% in the past several decades (Brahney et al., 2013).

Mineral dust influences climate both directly and indirectly. Dust in the atmosphere can affect Earth's radiative balance and act as cloud condensation nuclei resulting in cooling or warming of surface temperatures (Mahowald et al., 2006; Mahowald, 2011). Furthermore, dust can deliver key nutrients to ecosystems that have experienced intense chemical weathering or physical erosion, or have low concentrations of key nutrients in the parent material (Aciego et al., 2017; Kurtz et al., 2001; Pett-Ridge et al., 2009; Porder et al., 2007). Dust deposition can also alter precipitation pH (Brahney et al., 2013), and induce changes to lake water chemistry and biology (Brahney et al., 2014, 2015). In nutrient-limited deposition areas, dust can be an important source of critical nutrients (such as phosphorus, iron, and silicon) enhancing primary productivity or contributing pollutants to terrestrial ecosystems (Aciego et al., 2017; Arvin et al., 2017; Brahney et al., 2015; Coble et al., 2015; Dastrup et al., 2018; Jiao et al., 2018; Lybrand and Rasmussen, 2017; Ponette-Gonzalez et al., 2018). Therefore, dust is capable of acting as a fertilizer either increasing primary productivity or causing eutrophication when inputs are excessive. Understanding the effects of increasing desertification and the potential for heightened generation and transport of dust may aid in gauging the indirect effects of dust on the global carbon cycle.

Variations in dust production, transport, and deposition on long timescales are preserved in the paleoclimate record (Aarons et al., 2016; Neff et al., 2008), whereas more recent changes can be investigated through remote sensing (Evan et al., 2014, 2015) and ground-truth data collection using passive dust samplers (Aciego et al., 2017; Reheis et al., 2002; Reynolds et al., 2006b; Coble et al., 2015). Dust transport and variability is often closely linked to environmental conditions at the source area and atmospheric circulation regimes, and, because dust is a byproduct of weathering processes, it varies compositionally based on environmental conditions in source regions (Aarons et al., 2017a). This study leverages recently developed low blank and high precision radiogenic isotope techniques (Koornneef et al., 2014; Aarons et al., 2016) in an ongoing effort to document the dust cycle response to evolving climate conditions. In particular, we examine the spatial and temporal sensitivity of the dust cycle at sites along an elevational gradient in the southern Sierra Nevada of California. The results of the multiyear study are intended to serve as a calibration tool for predicting the regional biogeochemical response to increasing dust fluxes.

2. Background

2.1. Radiogenic isotopes as tracers of dust provenance

Variations in geologic history and ages imprint distinctive compositions of radiogenic isotopes of strontium (Sr) and neodymium (Nd) in rock, soil and dust, making them useful tools for distinguishing sediment and dust provenance (Biscaye et al., 1997; Grousset and Biscaye, 2005; Grousset et al., 1992). Measurements of Sr ($^{87}Sr/^{86}Sr$) and Nd ($^{143}Nd/^{144}Nd$) isotopes are traditionally used together to differentiate sediment source areas (host lithology) and are considered an excellent "fingerprinting" tool (Grousset and Biscaye, 2005; and references therein). Previous researchers have documented potential source area (PSA) Sr and Nd isotopic compositions in the Northern Hemisphere from minor and major contributors (Biscaye et al., 1997; Chen et al., 2007; Kanayama et al., 2002, 2005; Pourmand et al., 2014; Scheuvens et al., 2013), and more recent work has documented radiogenic (Sr, Nd, and hafnium) isotopic compositions of dust from western United States PSAs likely to generate large amounts of dust (Aarons et al., 2017a).

In a previous study, we investigated provenance using radiogenic isotope compositions and nutrient content of dust delivered to an elevational transect of the southern Sierra Nevada during a catastrophic drought year (2014). This was one of the first studies that applied both isotope and trace and major element geochemistry to trace dust sources and nutrient availability in modern dust samples throughout the course of a dry season, providing both temporal and spatial resolution to the regional dust cycle. During the 2014 season, radiogenic isotope compositions of deposited dust indicated that contributions from local sources in the Central Valley grew significantly as the summer dry period progressed from July to September (Aciego et al., 2017). This geochemical evidence coupled with major and trace elemental data suggested that a significant portion of dust and nutrients contributed to mid-elevation sites was attributable to an extreme regional drought. To probe the sensitivity of the dust cycle at these sites to regional and global droughts, we revisited the same elevational transect in 2015, during a period of ongoing drought in California and increasing drought in Asia. Documenting the variation of dust provenance during multiple years improves our understanding of the spatial and temporal differences in dust distribution during drought periods. Here, we present the results of the dust sampling campaign along the Southern Sierra Critical Zone Observatory (SSCZO) elevational transect in California, USA, during April-October of 2015. Below, we discuss the current and future research directions regarding geochemical analysis of aeolian dust.

2.2. Importance of ground-truthing nutrient inputs using geochemical measurements

The delivery of biologically important nutrients via weathering of rock surfaces is a key control on the presence and distribution of terrestrial life. Similar to the mechanical and chemical breakdown and transport of nutrients to the oceans via rivers, fine-grained dust can be uplifted into the atmosphere and transported to oceans and terrestrial biospheres. Therefore, documenting the dust cycle response to different climate scenarios is important to accurately predict the biogeochemical response to an increasing dust flux. While remote sensing data of dust uplift, transport, and deposition are available (Evan et al., 2014; Ginoux et al., 2012; Prospero et al., 2002), understanding the biogeochemical response to dust fertilization that spans a wide range of geochemical compositions and trace element concentrations is important to accurately reflect the carbon cycle response in Earth System model simulations.

Mineral dust deposition in oceans delivers nutrients such as Fe, which acts as a fertilizer for marine phytoplankton and is capable of altering global carbon dioxide (CO_2) concentrations (Jickells et al., 2005; Martin, 1990; Martínez-Garcia et al., 2014). The concentration of Fe in mineral dust can vary significantly based on the source area geochemistry, and the lability of Fe depends on its speciation (Hawkings et al., 2018; Schroth et al., 2009; Shoenfelt et al., 2017). Ferrous (Fe^{2+}) Fe is more bioavailable than ferric (Fe^{3+}) Fe, and the speciation of this macronutrient has a significant impact on marine (Shoenfelt et al., 2017) and likely terrestrial primary production. Previous studies relied on total dust and Fe fluxes to provide insight into the role of dust on CO_2 drawdown over long timescales (Martínez-Garcia et al., 2011, 2014), without considering the effect of Fe speciation on nutrient availability. Consequently, measurements of Fe speciation in atmospherically transported dust and its spatial variability are needed to quantify bioavailable nutrient concentrations. Global circulation models that include dust transport and deposition should consider Fe speciation to accurately predict the impacts on ocean fertilization and subsequent changes to the carbon cycle.

To quantify the role of mineral dust fertilization in the terrestrial realm, a study of sites along the SSCZO elevation gradient utilized a global compilation of erosion rates and modeled dust fluxes to show that dust deposition can serve as a large fraction of total soil inputs, especially in locations with slow erosion rates and long soil residence times (Arvin et al., 2017). Arvin et al. (2017) utilized Nd isotope

compositions of *Pinus jeffreyi* pine needles, dust, and bedrock at one of these sites to suggest that dust is the primary contributor of P in vegetation. The rationale behind using Nd isotopes as a tracer of P uptake and utilization lies in the chemical behavior of this element, which is a rare earth element (REE) that is concentrated in phosphate-bearing minerals (Chadwick et al., 1999). The incorporation of Nd into plants should therefore be a representative tracer of P uptake and utilization. Results from this site-specific study were broadened using a global data set of dust deposition and erosion rates, which indicated that dust is a significant driver of ecosystem evolution in eroding mountain landscapes (*i.e.*, mid-latitude montane ecosystems) likely reliant on dust derived nutrients (Arvin et al., 2017). The importance of ground-truthing geochemical observations and datasets lies in the ability to estimate the contribution of critical nutrients from exogenic dust, which varies significantly based on geochemical composition and is ultimately a function of geographical origin. Understanding the changes in nutrient export from areas that are rapidly undergoing increasing desertification and generating greater quantities of dust will become increasingly important with future climate change and land use intensification. The research described below is an effort to explore the temporal variability in dust sources and transport within the SSCZO.

2.3. Site description

Our study sites are located within the SSCZO, on the western slope of the Sierra Nevada, California, USA (Fig. 1). The sites include the San Joaquin Experimental Range (SJER; 400 m elevation), Soaproot (1100 m), Providence (2000 m), and Short Hair (2700 m). The region is characterized by a Mediterranean climate with cool, wet winters and warm, dry summers. It is common for the area to experience little to no precipitation during the summer growing season (mid-May to October), and the surrounding region was in the midst of an exceptional drought during 2012–2015, attributed to anthropogenic warming (Diffenbaugh et al., 2015). The drought in California extended into 2015, severely impacting the canopy water content of California forests and causing substantial ecological changes (Asner et al., 2016). In 2014, passive dust collectors were deployed (see Section 3.1 for more information) to both quantify dust flux and determine dust source provenance during the 2015 summer season along a ~2300 m elevational transect (Fig. 1). Dust samples were collected following a three-month deployment length in July and October 2015; information regarding collection date, location, sample name, elevation and deployment lengths are reported in Table 1. Dust flux rates were calculated using the dust masses at each site, the collector size, and deployment length.

2.4. Drought differences between 2014 and 2015

In 2014, California was in the midst of a catastrophic multi-year drought (US National Climate Data Center, 2014), which was longer and warmer than any other drought the state has experienced within the past millennium (Griffin and Anchukaitis, 2014) and resulted in the lowest 12-month accumulated precipitation in California in recorded history (Swain et al., 2014). From 2012 to 2016, the drought threatened California's surface water supplies, resulted in higher rates of groundwater extraction (Flint et al., 2018), led to massive forest die-off (Asner et al., 2016), and increased wildfire intensity (AghaKouchak et al., 2014; Diffenbaugh et al., 2015; Stephens et al., 2018; van Mantgem et al., 2013). Drought impacts deepened from 2014 to 2015 with respect to increased surface water shortage for agricultural activities, resulting in a ~33% increase in cropland fallowing from 2014 (Howitt et al., 2015). Annual statewide precipitation was higher in 2015 compared to 2014, however the annual statewide runoff was also higher (https://ca.water.usgs.gov/california-drought/california-drought-comparisons.html), suggesting that soil moisture levels may have been lower due to decreased infiltration. Low moisture soils are more vulnerable to erosion during prolonged periods without rainfall and can lead to increased dust transport (Prospero and Nees, 1986). This research aimed to test the sensitivity of annual changes in the regional drought upon local dust generation and transport. California's five-year-drought ceased following an anomalously wet 2016–2017 water year in California (California Department of Water Resources, 2018) which included extreme precipitation events (described as atmospheric rivers) during early 2017 (Cannon et al., 2018).

During the summer of 2014, large-scale circulation anomalies also led to the most severe drought of the past 60 years in north China and large areas of northeastern Asia (Wang and He, 2015). Dust from northern China has been identified previously as a contributor to the ecosystems of our study sites (Aciego et al., 2017). Data from the global Standardized Precipitation Evapotranspiration Index (SPEI) database indicates large areas of Mongolia, north China and northeastern Asia were under heightened drought conditions in July-October 2015 (Vicente-Serrano et al., 2010), which coincided with the sampling period described in this study.

Aciego et al. (2017), investigating provenance and nutrient content

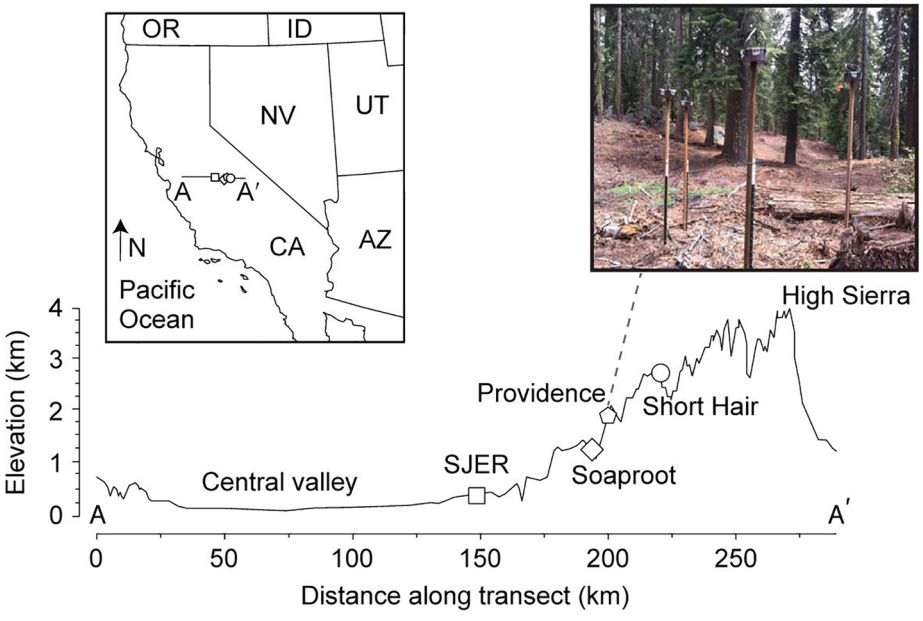

Fig. 1. Map and cross-section of the elevational-transect examined in this study, and a photograph of the Providence study site (adapted from Aciego et al., 2017). Regional map with study sites and cross-sectional transect show distribution of dust collection sites along the elevational transect. Note that site location symbols correspond to data symbols used in Figs. 2 and 3.

Table 1
Collection date, location, sample name, latitude and longitude, elevation and deployment length of samples analyzed in this study.

Collection date	Location	Sample Name	Latitude	Longitude	Elevation (m)	deployment length (days)
7/20/15	SJER	J1-J	37.10794	−119.73198	400	103
7/20/15	SJER	J3-J	37.10794	−119.73198	400	103
7/20/15	Soaproot	T3-J	37.03053	−119.25817	1100	105
7/20/15	Soaproot	T6-J	37.03053	−119.25817	1100	105
7/20/15	Providence	P2-J	37.06008	−119.18268	2000	105
7/20/15	Providence	P4-J	37.06008	−119.18268	2000	105
7/19/15	Shorthair	S2-J	37.06698	−118.987107	2700	104
7/19/15	Shorthair	S3-J	37.06698	−118.987107	2700	104
10/10/15	SJER	J1-O	37.10794	−119.73198	400	87
10/10/15	SJER	J2-O	37.10794	−119.73198	400	87
10/10/15	SJER	J3-O	37.10794	−119.73198	400	87
10/8/15	Soaproot	T2-O	37.03053	−119.25817	1100	85
10/8/15	Soaproot	T3-O	37.03053	−119.25817	1100	85
10/8/15	Soaproot	T6-O	37.03053	−119.25817	1100	85
10/8/15	Providence	P1-O	37.06008	−119.18268	2000	85
10/8/15	Providence	P2-O	37.06008	−119.18268	2000	85
10/8/15	Providence	P4-O	37.06008	−119.18268	2000	85
10/7/15	Short Hair	S2-O	37.06698	−118.987107	2700	84
10/7/15	Short Hair	S3-O	37.06698	−118.987107	2700	84
10/7/15	Short Hair	S5-O	37.06698	−118.987107	2700	84

of dust delivered along this SSCZO elevational gradient, found that contributions of dust from the Central Valley grew considerably during the summer dry period, suggesting that a significant portion of dust and nutrients was attributable to the extreme regional drought in California. To probe the sensitivity of the dust cycle to both regional and global droughts, we conducted a dust sampling campaign along the same elevational transect in 2015, a period of ongoing drought in California and increasing drought in Asia.

3. Methods

3.1. Sample collection

We collected dust samples using a passive collection method previously described in Aciego et al. (2017) at four elevations along the SSCZO gradient (Fig. 1). Briefly, the passive collectors consisted of Teflon-coated round pans (25.4 cm in diameter) filled with quartz marbles that were suspended from the pan bottom with kevlar mesh. All materials in contact with the dust (pan, marbles, and mesh) were pre-cleaned prior to field installation using bleach, distilled 2 M HCl, and distilled 3 M HNO_3 with rinses of > 18.2 MΩ water between each cleaning step. The collectors (five at each site) were deployed on ~2-m tall wooden posts in open areas at each field site to avoid contribution of locally derived sediment. Collectors were initially deployed at all sites between April 1–4, 2015, with the first sample collection taking place July 15, 2015, resulting in a deployment length of 103–105 days. The collectors were subsequently re-deployed on July 15, 2015 and the second sample collection occurred on October 7 (Short Hair), 8 (Providence and Soaproot) and 10 (San Joaquin Experimental Range; SJER), 2015 with deployment lengths of 84–87 days. Specific details regarding sample collection are reported in Table 1.

3.2. Sample processing

To recover and archive dust samples from each collector on the dates listed above, we rinsed the marbles with > 18.2 MΩ water into the Teflon-coated pan. After removing the marbles and mesh from the pan, we transferred the water and suspended dust to pre-acid cleaned and sterilized 1 L LDPE Nalgene bottles. Samples were frozen until filtering to prevent any leaching between dust and water. Samples were melted and immediately filtered to exclude the soluble contribution (*e.g.,* sea salt aerosols) using consecutive 30 and 0.2 μm polycarbonate membrane filters. Following filtration, the samples were weighed for dust mass and then the dust was dissolved directly off of the 0.2 μm filter using techniques previously described in Aciego et al. (2009). Finally, the insoluble dust fraction was chemically separated with ion exchange columns and Eichrom resins using procedures outlined in Koornneef et al. (2015). A 10% aliquot of each sample was taken for trace element analysis, described below in Section 3.4.

3.3. Radiogenic isotope analysis

Samples were measured for Nd and Sr isotopic compositions on a Thermo Scientific Triton *Plus* thermal ionization mass spectrometer (TIMS) at the Vrije Universiteit, Amsterdam, The Netherlands. The TIMS was equipped with 10^{11} Ohm resistors for Sr and most Nd isotope ratios, however low Nd concentration dust samples (S2-J and S3-J) along with a basalt rock standard (BCR-2) were measured using 10^{13} Ohm resistors for $^{143}Nd/^{144}Nd$ ratios. Instrumental mass fractionation for Nd was corrected using the exponential law and a $^{146}Nd/^{144}Nd$ value of 0.7219 and for samples measured with 10^{11} Ohm resistors and the low-noise 10^{13} Ohm resistors mass 147 was monitored for potential Sm interference (Koornneef et al., 2014). The reference standard JNdi-1 was measured concurrently with the samples ($^{143}Nd/^{144}Nd$ = 0.512102 ± 0.000007 2σ, n = 2). Sr measurements were normalized to $^{88}Sr/^{86}Sr$ = 8.375209 to account for mass bias. The Sr isotopic standard NBS-SRM-987 was also measured with the samples ($^{87}Sr/^{86}Sr$ = 0.710243 ± 0.000010 2σ, n = 2).

To ensure adequate chemical digestion and ion-exchange separation, two < 10 mg aliquots of the United States Geological Survey (USGS) BCR-2 basalt rock standards were digested, separated, and measured for Sr and Nd isotopic composition. The BCR-2 aliquots contained ~900–1200 ng of Sr and ~6–8 ng of Nd. The average Nd isotopic composition of BCR-2 was $^{143}Nd/^{144}Nd$ = 0.512631 (2σ = 0.000019, n = 2) and the average Sr isotopic composition was $^{87}Sr/^{86}Sr$ = 0.705014 (2σ = 0.000010, n = 2), in good agreement with other reported literature values of $^{143}Nd/^{144}Nd$ = 0.512637 and $^{87}Sr/^{86}Sr$ = 0.705000 (Jweda et al., 2015). All Nd isotope compositions are reported here as ε_{Nd}, which is defined as: $\varepsilon_{Nd} = ([(^{143}Nd/^{144}Nd)_{sample}/(^{143}Nd/^{144}Nd)_{CHUR}]) - 1 \times 10^4$, where $^{143}Nd/^{144}Nd)_{CHUR}$ is the Nd isotopic composition of the Chondritic Uniform Reservoir (CHUR; Jacobsen and Wasserberg, 1980). Radiogenic isotope compositions of 2014 and 2015 dust at the SSCZO sites are presented in Figs. 2 and 3.

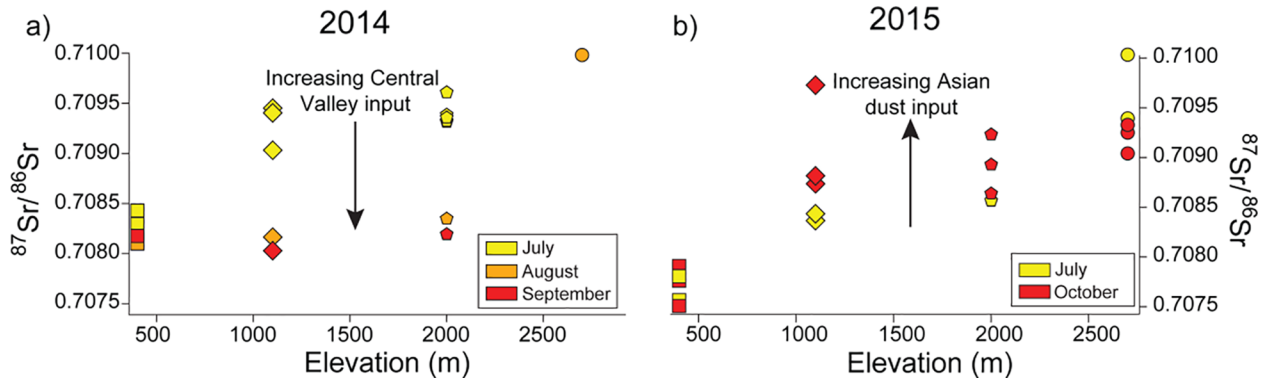

Fig. 2. Strontium isotope compositions of a) 2014 (Aciego et al., 2017) and b) 2015 (this study) dust samples at the four sites plotted as a function of elevation. Symbols for four sites match those in Fig. 1. Colors are indicative of timing of sample collection during the sampling interval. For 2014: yellow (July), orange (August), and red (September). For 2015: yellow (July), and red (October). Note that trends throughout the summer dry season are opposite for 2014 compared to 2015.

3.4. Trace element analysis

Aliquots of each sample were measured for trace element concentrations (P, S, Na, Al, Cr, Mn, Fe, Ni, Cu, Zn, Sr, Rb, Nd, Sm, Th, and U) on a Nu Instruments Attom high-resolution inductively coupled plasma mass spectrometer at the University of California Irvine. Samples were diluted in 2% HNO_3 and blanks, standards, and samples were spiked with a mixed internal standard (1 ppb In, Sc) prior to analysis. Concentrations were calculated from drift-corrected intensities of four external standards of known concentration. The total procedural blank accounts for up to 10% of the concentration measured. Macro, micronutrient and raw sample concentrations are reported in Table S1. Heavy metal concentrations in Fig. 3 are reported as the crustal enrichment factor (EF). The crustal EF is defined as the concentration ratio of an element relative to that of aluminum (Al, which is representative of rock and soil dust) in the dust sample, normalized to the concentration ratio found in the upper continental crust (UCC) (Wedepohl, 1995). For examples, the crustal EF for zinc (Zn) is: $([Zn]_{sample}/[Al]_{sample})/([Zn]_{UCC}/[Al]_{UCC})$.

3.5. Isotope mixing model

We used the following two endmember isotope-mixing models (as modified from White 2013) to determine the relative inputs of Central Valley-derived dust versus Asian-derived dust needed to achieve the observed Sr-Nd isotope compositions of the SSCZO dust:

$$^{87}Sr/^{86}Sr_M = [^{87}Sr/^{86}Sr_A \times f \times (Sr_A/Sr_M)] + [^{87}Sr/^{86}Sr_B \times (1 - f) \times (Sr_B/Sr_M)],$$

where $^{87}Sr/^{86}Sr_M$ is the Sr isotope composition of the modeled mixed

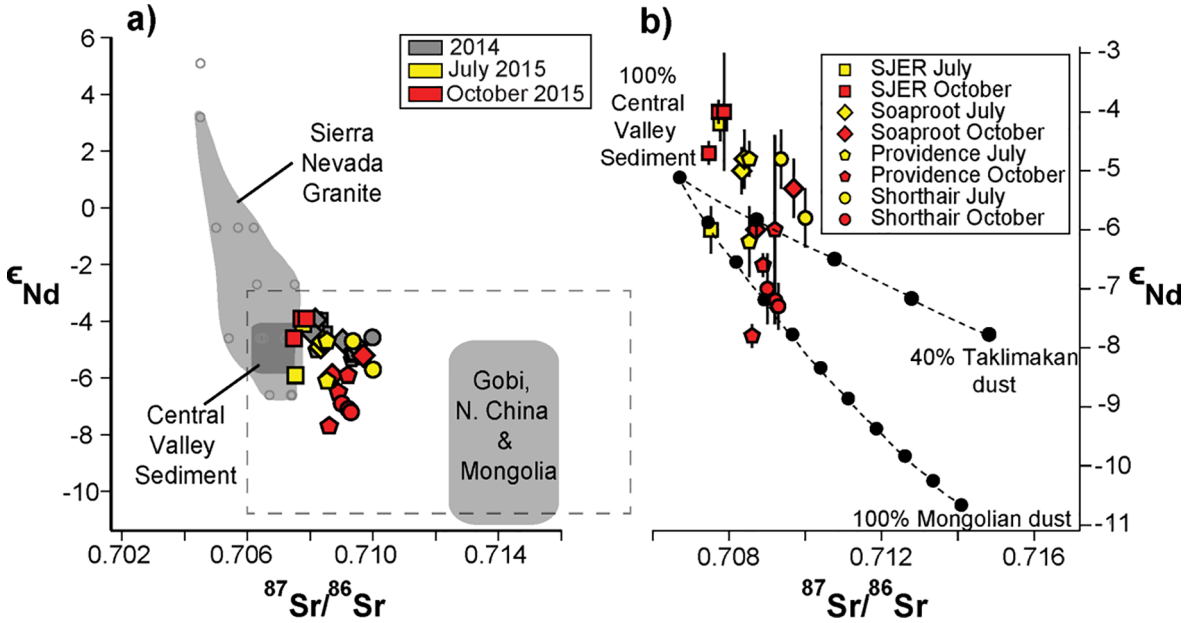

Fig. 3. Combined Sr and Nd isotopic compositions of dust from the SSCZO study sites during 2014 (Aciego et al., 2017) and 2015 (this study) years. a) Sr and Nd isotopic compositions of 2014 dust (gray symbols) with respect to 2015 dust during July (yellow symbols) and October (red symbols) sampling periods. Also shown are Sr and Nd isotopic compositions of hypothesized potential source areas of dust: Central Valley sediment (Ingram and Lin, 2002; Rosenbauer et al., 2013), Sierra Nevada granite (Rotberg, 2008), and a compilation of data from the Gobi, Northern China, and deserts of outer Mongolia (Biscaye et al., 1997; Chen et al., 2007; Kanayama et al., 2002) are also shown. For clarity, error bars on isotope data are not shown. Gray dashed box indicates area shown in panel (b). b) Sr and Nd isotopic compositions of 2015 dust (this study) with isotope mixing model results for a mixture of Central Valley sediment with Mongolian and Taklimakan desert dust, respectively. Black circles along dashed lines are 10% increments in dust contribution from two-endmember mixing. Strontium isotope errors (± 2 SE) are smaller than symbol size and Nd isotope errors (± 2 SE) are shown.

dust, $^{87}Sr/^{86}Sr_A$ and $^{87}Sr/^{86}Sr_B$ are the isotope compositions of the Central Valley (0.7067; Ingram and Lin, 2002) and Asian dust (Mongolian and Taklimakan dust) endmembers, respectively (0.714 and 0.727; Aciego et al., 2017), f is the proportion of the Central Valley component in the mixture, Sr_A and Sr_B are the concentrations of Sr in the Central Valley and Asian dust endmembers, respectively (both estimated 100 ppm based on data from Ingram and Lin, 2002; Yokoo et al., 2004), and Sr_M is the concentration of strontium in the mixed dust ($Sr_M = Sr_A * f + Sr_B * (1 - f)$).

For Nd isotopic compositions of the mixed dust we use the following equation:

$$^{143}Nd/^{144}Nd_M = [^{143}Nd/^{144}Nd_A \times f\,(Nd_A/Nd_M)] + [^{143}Nd/^{144}Nd_B \times (1 - f) \times (Nd_B/Nd_M)],$$

where $^{143}Nd/^{144}Nd_M$ is the calculated neodymium isotope composition of the mixed dust, $^{143}Nd/^{144}Nd_A$ and $^{143}Nd/^{144}Nd_B$ are the isotope compositions of the Central Valley (0.51238; Rosenbauer et al., 2013) and Asian dust endmembers, respectively (0.512095; Yokoo et al., 2004), f is proportion of the Central Valley component in the mixture, Nd_A and Nd_B are the concentrations of Nd in the Central Valley and Asian dust endmembers, respectively (16.8 and 23.25 ppm; Rosenbauer et al., 2013; Yokoo et al., 2004), and Nd_M is the concentration of neodymium in the mixed dust ($Nd_M = Nd_A \times f + Nd_B \times (1 - f)$). The results of the isotope-mixing models are shown in Fig. 3b.

4. Results

4.1. Strontium isotope compositions

The $^{87}Sr/^{86}Sr$ isotopic composition of the 2015 dust samples lies within the range of 0.707472 to 0.710000 (Table S1). Strontium isotope compositions from 2015 dust correlate positively ($r^2 = 0.64$, $n = 20$) with elevation (Fig. 2a,b), indicating a strong influence of regional dust sources at lower elevations and verifying the connection between regional climate and dust generation. The average shift in the $^{87}Sr/^{86}Sr$ ratio between July and October samples is > 140 ppm, where July and October samples yield average $^{87}Sr/^{86}Sr$ ratios of 0.708557 and 0.708705, respectively. The more radiogenic (higher) $^{87}Sr/^{86}Sr$ ratios in October 2015 may be indicative of increasing Asian dust input throughout the season, coinciding with a significant drought period sustained throughout East Asia and Mongolia.

While spatial patterns of Sr isotope compositions of dust between 2014 and 2015 are in agreement with higher $^{87}Sr/^{86}Sr$ ratios with increasing elevation, the temporal patterns differ. Throughout the dry season in 2014, Aciego et al. (2017) observed a decrease in Sr isotope compositions (Fig. 2a), most pronounced at the mid-elevation sites, suggesting increasing input of Central Valley dust with prolonged drought. In contrast, the 2015 dry season shows an increase in Sr isotope compositions at the three lowest elevation sites (Fig. 2b) between July and October. This change in dust composition suggests an increasing Asian dust input because Asian dust is typically more radiogenic (Biscaye et al., 1997; Chen et al., 2007; Kanayama et al., 2002) compared to the composition of regional Central Valley dust (Rosenbauer et al., 2013). These results reflect regional and global variations in the dust cycle, with implications for predicting future dust inputs to nutrient-poor areas under climate change and increasing drought intensity.

The Nd isotopic composition of the 2015 dust samples lies within the range of $\varepsilon_{Nd} = -3.9$ to -7.7 (Table S1). There does not appear to be a significant shift in the average Nd isotopic composition of dust collected in July versus October, which ranged from $\varepsilon_{Nd} = -5.1$ to -5.9 respectively. However, the most significant shifts in Nd isotopic compositions are observed at the highest elevation sites. For the Providence and Short Hair sites (elevation 2000 and 2700 m.a.s.l., respectively), the average Nd isotope compositions during July was $\varepsilon_{Nd} = -5.3$ and during October was $\varepsilon_{Nd} = -6.9$, with the October Nd isotope composition consistent with the interpretation of increasing relative input of Asian dust sources throughout the dry season (Chen et al., 2007; Kanayama et al., 2002).

4.2. Differences in dust provenance between 2014 and 2015

The prevailing wind direction at the SSCZO is west-to-east (see Figs. S1–S7), suggesting that the majority of atmospherically transported dust reaching this region originates from the west. HYSPLIT back trajectory analysis (see Section 5.1) indicates that air masses originate from local areas ranging from throughout California to areas within the western United States, to transoceanic sources (Figs. S1–S7). The most likely regional sources of dust deposited at the SSCZO are Central Valley sediments that are derived from the Coast Ranges in California and the local granitic batholith of the Sierra Nevada, or the deserts in Asia. Asian dust travels across the Pacific Ocean via westerly winds (Duce et al., 1980; Wilkening et al., 2000), and is capable of reaching North America (Ault et al., 2011; Husar et al., 2001). Major Asian dust source regions include the Taklimakan Desert, Gobi Desert, and Loess Plateau of China, which account for ~25% of global dust emissions (Ginoux et al., 2004). The combined Sr-Nd isotope compositions of the 2014 and 2015 dust are shown in Fig. 3a. The 2015 dust spans a greater range in Nd isotope compositions, suggesting a change in dust source(s) transported to the SSCZO between 2014 and 2015. In particular, the samples collected in October 2015 from the two highest elevation sites (Providence and Short Hair) display the most non-radiogenic (negative) Nd isotope compositions.

Isotope-mixing models can aid in distinguishing relative inputs from dust sources, with Central Valley sediment serving as one endmember and Mongolian and Taklimakan dust serving as separate endmembers (Fig. 3b). When the 2015 SSCZO dust isotope data is viewed in the context of the isotope-mixing model, the results indicate a difference from nearly 100% Central Valley sediment input at the lowest elevation site (SJER) to between 30 and 40% input from a Mongolian dust endmember source at the highest elevation site (Short Hair). In addition to the spatial variability, the two high elevation sites (Providence and Short Hair) shift from between ~80–90% Central Valley sediment input in July to ~60–80% Central Valley sediment input in October 2015 (Fig. 3b). These sites appear to receive a corresponding 10–40% increase of Asian dust from July to October.

4.3. Dust supply rate and P flux

The dust supply rates to the SSCZO sites during the duration of the 2014 and 2015 dry seasons are reported in Fig. 4a, with extrapolated P flux from raw concentration measurements shown in Fig. 4b. The dust supply rates during 2014 and 2015 span several orders of magnitude, with the highest variance between the two years at the lowest and highest elevation sites, respectively. Variations in dust supply rates at each site throughout the sampling period were observed both in 2014 and in 2015, most notably at the lowest (SJER) and highest (Short Hair) elevation sites (Fig. 5a). Passive dust collectors were stationed in strategically open areas to avoid vegetation blocking dust deposition, and each dust collector was located ~2 m apart. Variations in dust flux at these sites may be a result of small-scale differences among the passive dust collector locations, post-depositional processes, or both. The dust supply rate to all sites was significantly higher in 2014, which is likely due to heightened dust input from the Central Valley coinciding with the increasing California drought severity. The P flux to the sites was higher in 2014 compared to 2015 as this is dependent upon dust supply rate and raw P concentration of dust samples. There is no clear systematic trend of dust supply rate in 2014 or 2015 with respect to elevation. The average dust supply rates at the sites in July versus October, respectively, are as follows: SJER—0.07 and 3.35 $g\,m^{-2}\,a^{-1}$, Soaproot—1.31 and 1.99 $g\,m^{-2}\,a^{-1}$, Providence—1.23 and 1.91 $g\,m^{-2}\,a^{-1}$,

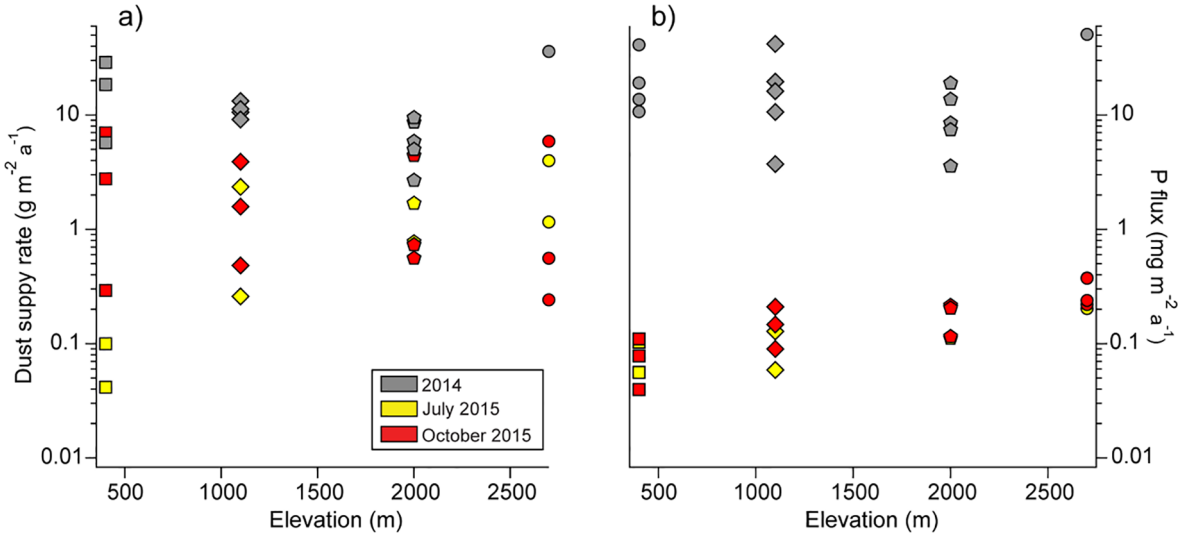

Fig. 4. Dust supply rates and P fluxes to the SSCZO study sites during 2014 (Aciego et al., 2017) and 2015 (this study) years. a) Dust supply rates of 2014 dust (gray symbols) with respect to 2015 dust during July (yellow symbols) and October (red symbols) sampling periods b) Phosphorus fluxes of 2014 (Aciego et al., 2017) and 2015 dust (this study). Note y-axes are in log scale.

and Short Hair—2.57 and 2.23 $g\,m^{-2}\,a^{-1}$. The average dust supply rates (and P flux) at all the SSCZO sites (except the highest elevation site Short Hair) are higher in October versus July, suggesting a more pronounced dust transport later in the dry season. Based on the radiogenic Sr and Nd isotope compositions of the dust delivered to the SSCZO sites, it is most likely that the dust in the later portion of the sampling period is dominated by input from Asian deserts, however it is difficult to attribute an increase in Asian dust supply based solely on isotope and flux data. The large differences in dust supply rates and P flux between the 2014 and 2015 dry seasons highlights the variability of the dust cycle at these temperate montane sites.

4.4. Trace element concentrations

A selection of macro- (Mg, sulfur (S), P) and micronutrient (Fe) concentrations of dust delivered to the SSCZO sites are reported in Fig. 5, after normalization to the average UCC concentrations (Wedepohl, 1995). The majority of dust samples are lower in concentration than the average UCC compositions (Fig. 5), suggesting that chemical reactions during atmospheric transport alter or dissolve mineral species, which has been noted in particular for P (Stockdale et al., 2016) and Fe (Baker and Croot, 2010; Spokes et al., 1994).

Several heavy metal (Cr, Ni, Cu and Zn) concentrations are reported as crustal EF in Fig. 5b. The crustal EF compares the relative concentration of an analyte in a material (in this case mineral dust) to that in soil or sediment (in this case average UCC concentration). All heavy metal concentrations, with the exception of Cr, are higher than the average UCC concentration, suggesting significant contributions from an alternative source such as volcanoes, forest fires, or anthropogenic activity. Anthropogenic Cr, Ni, Cu, and Zn primarily originate from industrial processes such as the combustion of fossil fuels, nonferrous metal production, steel and Fe manufacturing, and waste incineration (Nriagu and Pacyna, 1988). Zinc was emitted to the atmosphere at the highest rate of all heavy metals (with the exception of lead) by the late 1980s (Nriagu and Pacyna, 1988), and is found to have the highest concentration in the dust samples measured here. More recent studies of toxic heavy metals in the environment observed increases in Cr and Ni concentrations up to 16 and 13 fold between 1941 and 2012 (Martin et al., 2015). In addition, the concentrations of anthropogenic metals, such as Cr and Zn, have also increased in ambient air due to rapid

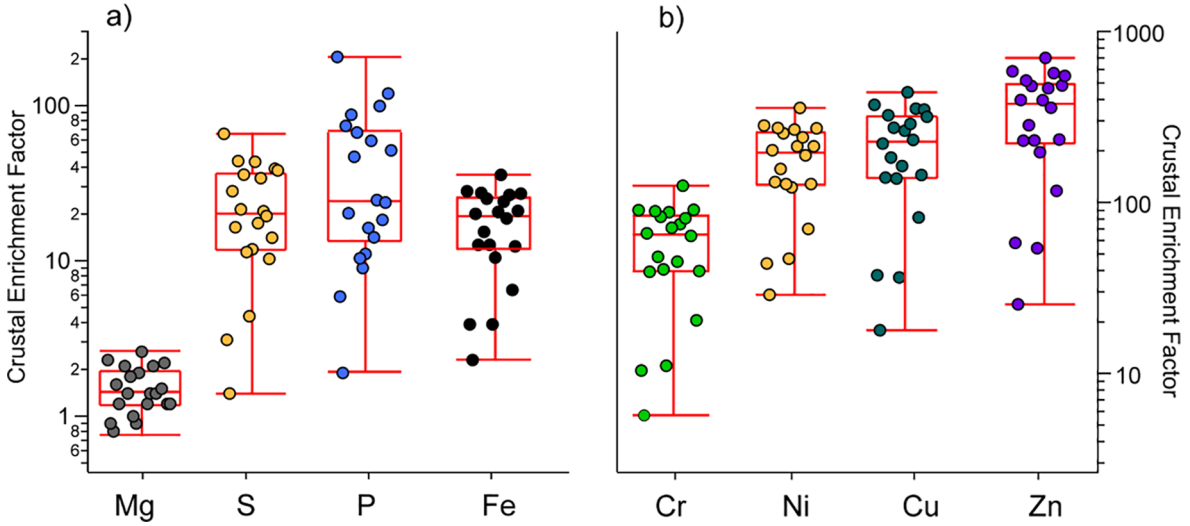

Fig. 5. Spear style box-and-whisker plot showing trace element concentrations of individual dust samples measured in this study. a) Macro-and micro-nutrient concentrations of dust samples reported as Crustal Enrichment Factor. b) Heavy metal concentrations reported as Crustal Enrichment Factor.

urbanization and industrialization (Suvarapu and Baek, 2017). The high concentrations of heavy metals found here could be a result of adsorption processes onto clay mineral surfaces (Uddin, 2017), and may have biogeochemical implications as they can accumulate in plants and animals and enter humans through the food chain.

5. Discussion

5.1. Wind directions at SSCZO site: insights from HYSPLIT back trajectory analysis

Back trajectory analysis is a useful tool for tracing atmospherically transported aerosols, and can provide more information regarding the likely source areas of dust transported to the SSCZO site during the study period. Here we use the web-based version of the model (HYbrid Single-Particle Lagrangian Integrated Trajectory Model, 1997, http://www.arl.noaa.gov/ready/hysplit4.html) to determine the backward air trajectories at several altitudes (500, 5000, 10,000 m.a.s.l.) ending at the four SSCZO sites during all weeks throughout the sampling period (see Figs. S1–S7 in Supplementary Information). The HYSPLIT model computes air parcel trajectories and illustrates dispersion and deposition pathways (Draxler and Hess, 1998) using publicly available model-derived meteorological data formatted for HYSPLIT from NOAA ARL (www.ready.noaa.gov/archives.php) and NOAA NCEP (ftp://ftpprd.ncep.noaa.gov//pub/data/nccf/com/hysplit/prod/). Similar to the methods outlined in Aciego et al. (2017), the HYSPLIT back trajectories were initiated every 12 h starting 315 h prior to 12:00 UTC time each week in April, May, June, July, August, September, and the first 2 weeks in October 2015. There may be errors up to 20% in the accuracy of the trajectories due to the resolution of the wind field data and meteorology (Stohl, 1998), however they are used here for comparing the radiogenic isotope composition of mineral dust deposited at the SSCZO site to atmospheric transport patterns.

The back trajectories from each of the four sites during April 2015 are variable based on the week, however there is a general trend of air masses originating from transoceanic locations from weeks 1–3, whereas weeks 4–5 are more localized (Fig. S1). It possible that during weeks 4–5 the dust transported from air masses originating from the southwest United States is from the Mojave Desert, which is supported by radiogenic isotope compositions of potential source area dust from within that region (Aarons et al., 2017b). In week 1, the trend of air mass distance and elevation of the site is evident, as the highest elevation site (Short Hair, 2700 m.a.s.l) receives air masses traveling at higher altitudes in the atmosphere and longer distances. In contrast, the back trajectories during May 2015 are almost entirely originating from local or regional locations (Fig. S2). Dust transported to the SSCZO sites during this time period may be more originating from locally identified sources such as the Central Valley (with sediment derived from the Coast Ranges and the Sierra Nevada Mountains). The back trajectories from June 2015 are similar to May 2015, with most air masses originating from local or regional sources in the southwest United States (Fig. S3). During the first 2 weeks of July 2015, air masses are originating almost solely from the southwest United States, and some transport from a southwesterly direction across the Pacific Ocean (Fig. S4). The first sample collection occurred during the second week of July and, based on the results of the back trajectory analysis, it is likely that the dust transported during the first portion of the sampling campaign originated from local or regional sources.

Weeks 3–5 of July 2015 are variable with air masses originating from both local and transoceanic locations, however, the prevailing winds appear to be in a W-E direction (Fig. S4). In August 2015, week 1 experienced air masses originating from California, Nevada, Arizona and New Mexico (Fig. S5). Week 3 in August 2015 experienced air masses originating from both local and long-range sites, as evidenced by the high and low elevations of the air mass trajectories reaching each site. In September 2015 the air mass trajectories in all weeks are highly variable (Fig. S6), ranging from transoceanic in weeks 1, 3, 4, and 5, and very localized in week 2. Additionally, during week 4, there appears to be more variability in the air mass transport with respect to site elevation. The pattern observed during this week is opposite that expected, with more global transport at the lower elevation sites and more localized transport at the highest elevation site. The second sample collection occurred during the transition between the first and second week of October 2015, with week 1 experiencing air mass transported from solely long range sites and week 2 experiencing air mass transport primarily from the east (Fig. S7).

While it is difficult to attribute air mass transport directions to specific source area sites, it is clear from the back trajectory analysis that the wind transport is primarily from the W-E, with some instances of dust transported from local southwestern areas of the United States. Increased dust transport from the southwestern United States would shift the Sr isotope compositions of the dust towards more radiogenic compositions, and more negative Nd isotope compositions. Throughout the sampling period, air masses from both local and transoceanic sources are reaching the SSCZO sites. It is likely that the air masses originating from across the Pacific Ocean are transporting Asian dust, and is supported based on the Sr-Nd isotope compositions of the dust collected at the SSCZO sites. Future work should incorporate size distribution of dust particles, as this is another indicator of regional versus globally transported dust (Aarons et al., 2017a; Delmonte et al., 2002), as well as hafnium isotope measurements of the dust particles, as this has been shown to scale with distance from the dust source region (Aarons et al., 2013). Another important consideration is the potential contribution of trace and major elements from organic particles such as pollen.

5.2. Neodymium isotope compositions from Sierra Nevada granite

The provenance of dust samples from the 2014 sampling period were determined by comparing the measured Sr-Nd isotopic compositions of dust to likely potential source areas (Aciego et al., 2017). The most likely local to regional source areas were identified as local granitic bedrock of the Sierra Nevada and sediments from the Central Valley derived from the Coast Ranges. To evaluate the possibility of local dust contribution via eddies driving material from the ground to the dust collectors located ~2 m above ground, the Sr-Nd composition of the dust was evaluated in the context of Sierra Nevada granite bedrock compositions (DePaolo, 1981). Aciego et al. (2017) excluded the possibility of contribution from Sierra Nevada granite based on the Sr isotope ratios of the dust ($^{87}Sr/^{86}Sr$ = 0.708 to 0.710) and the corresponding ε_{Nd} compositions at this range (dust ε_{Nd} = −5.5 to −4.2 and Sierra Nevada granite = −10 to −25). One issue associated with using this dataset from DePaolo (1981) is the difference in normalization procedures for the raw Nd isotope data.

Volatilization and ionization during mass spectrometry results in the breaking of chemical bonds, which is mass dependent. Therefore, heating and evaporation of a sample will lead to mass-dependent fractionation, resulting in the preferential evaporation of lighter isotopes first. This fractionation effect leads to the observed isotopic composition of the sample becoming progressively heavier throughout the sample measurement. To account for instrumental mass fractionation during heating and ionization of Nd, the raw radiogenic isotope data are normalized to the ratio of stable Nd isotopes. For Nd, masses of evaporating ions are normalized to and corrected using the exponential law and an internationally agreed upon $^{146}Nd/^{144}Nd$ value of 0.7219 (O'Nions et al., 1979). The ε_{Nd} range of Sierra Nevada granite obtained from DePaolo (1981) was normalized to a ratio of $^{146}Nd/^{142}Nd$ = 0.63613, which is different than what was used while measuring dust samples in the 2014 study (Aciego et al., 2017) and in this study. Therefore, the data from DePaolo (1981) cannot be used to discern whether locally sourced granite sediment contributed to the observed dust compositions and has not been used in this study.

We can evaluate whether Sierra Nevada granite was a significant contributor of dust to the 2014 and 2015 sampling periods by utilizing Sr-Nd isotope compositions from the Sierra Nevada granite and granodiorite (Rotberg, 2008) normalized to the $^{146}Nd/^{144}Nd$ value of 0.7219 (O'Nions et al., 1979), as an alternative to the Nd isotope compositions reported in DePaolo (1981). While none of the 2014 dust samples lie within the Sierra Nevada granite source array, several samples from the 2015 season plot within the periphery of this array but also within the Central Valley source array (Fig. 3a). Specifically, the samples are from the lowest elevation site (SJER, 400 m.a.s.l), which based on its proximity to the Central Valley is likely sediment derived from the Sierra Nevada granite and nearby Coast Ranges. While physical size sorting of sediment and dust during atmospheric transport may affect the radiogenic isotope compositions of dust transported to the SSCZO sites, it is unlikely that this is the cause of the range in Nd isotope compositions observed in the 2014 or 2015 samples.

5.3. Potential for variations in isotope compositions of dust due to physical size sorting

Previous research has demonstrated that fractionation of Sr isotopes of mineral dust during atmospheric transport can occur due to size sorting (Aarons et al., 2013), likely a result of mineralogical differences between fine and coarse grained particles. Specifically, fine-grained particles are typically more radiogenic with respect to Sr compared to the coarse grained particles due to mineralogical differences between size fractions. Fine-grained dust may contain a higher Rb/Sr ratio due to a larger proportion of secondary minerals such as phyllosilicates and micas, which have more radiogenic Sr isotope compositions (Blum and Erel, 1997; Stewart et al., 2001). Conversely, Nd isotopes have been noted for their congruent isotopic compositions during physical and chemical weathering processes in mineral dust and suspended sediment (Frank, 2002; Goldstein et al., 1984). More recent work investigating *trans*-Atlantic mineral dust noted no relationship between Sr and Nd isotopic compositions and dust particle size (van der Does et al., 2018), therefore it is important to take into account the possibility of size sorting exhibiting a control on the observed Sr-Nd isotope compositions of dust in this study.

One possibility is that the Sr isotope variability observed in the mineral dust transported to the SSCZO sites is a result of particle sorting during atmospheric transport. However, we would expect the Nd isotope composition of mineral dust to remain constant, as it is unaffected by changes in mineralogy and size sorting (Aarons et al., 2013; Kanayama et al., 2005) and should be a recorder of the source "fingerprint" rather than secondary processes. In the case of the dust observed at the sites during the 2014 and 2015 dry seasons, both sets of samples plot outside of the Central Valley and Sierra Nevada granite source array (Fig. 3), and span a relatively large range in Nd isotope compositions. In particular, the samples from the 2015 season range from $\varepsilon_{Nd} = -7.7$ to -3.9, which cannot be explained as a result of size sorting of Central Valley sediment, and is more likely a result of mixing between local (*e.g.,* Central Valley or Sierra Nevada granite) and long-range (*e.g.,* Asian dust sources) transported dust.

5.4. Implications of increased drought frequency in Asia on North American dust cycle

Based on the results of the 2015 summer dry season and previous studies (Ault et al., 2011; Vicars and Sickman, 2011; Aciego et al., 2017), dust from Asia could be a significant contributor of potentially viable nutrients to the SSCZO and likely much of the western slopes of the Sierra Nevada. Understanding the relationship among drought frequency and intensity, water availability, and land and soil degradation in Asia and the generation and transport of dust should aid in predicting future rates of dust flux to the western United States. East Asia is a region highly impacted by and subject to extreme drought conditions, with the regions of north and southwest China experiencing the highest drought frequencies and longest durations within Asia (Zhang and Zhou, 2015). Although east Asian precipitation is poorly simulated in current climate models, predictions of atmospheric circulation patterns indicate increasing drought frequency and intensity over southeastern Asia under heightened CO_2 conditions (Zhang and Zhou, 2015). Spatiotemporal data describing droughts throughout central Asia depict longer average drought duration and higher drought severity between 2003 and 2015, which could lead to soil and land degradation and potentially strengthen dust generation and transport from this region to North America (Guo et al., 2018).

Currently, there is limited systematic research on the generation and transport of *trans*-Pacific dust from Mongolian grasslands, which has a documented correlation between increased dust event frequency and drought periods, and suggesting that dust emissions from Mongolia are related to surface dryness (Munkhtsetseg et al., 2016). In the past decade, the Mongolian Plateau has experienced drought that was considered highly unusual (but not unprecedented) over 2000 years in terms of severity and duration (Hessl et al., 2018), and could result in heightened dust transport from the Gobi Desert. Studies probing the role of soil moisture on dust events and transport indicate that as wind speed increases, the probability of dust outbreaks becomes strongly dependent on soil moisture (Kim and Choi, 2015). Thus, there appears to be a strong reliance of dust generation and transport on soil moisture conditions, which may result in heightened *trans*-Pacific dust transport with increasing drought conditions in East Asia.

6. Conclusions

Recent research suggests terrestrial primary productivity can be stimulated by dust fertilization, which is a key driver in ecosystem development and landscape evolution. Documenting the response of the dust cycle to a changing climate scenario and providing ground-truthing physical and geochemical measurements enhance climate model predictions of biogeochemical responses to increasing dust flux or changes in dust sources. This study explored the temporal sensitivity of the dust cycle with respect to regional and global droughts. The results suggest that severe droughts in *trans*-oceanic locations have the potential to supplement the trace element delivery to sites that may be nutrient limited. The two high elevation sites (Providence and Short Hair) experienced an increase in Asian dust delivery from between ~10–20% in July to ~20–40% in October, and coincided with intensifying drought throughout Asia. Measurements of dust particle diameter together with hafnium isotope compositions would provide another line of evidence for distinguishing between local versus globally transported dust to the SSCZO sites. Dust can be a significant contributor in ecosystems that are nutrient limited due to intense weathering regimes, fast physical erosion rates, or low concentrations of nutrients supplied by bedrock. Identifying and quantifying the locations and ecosystems where dust is a potentially significant driver of primary productivity, and assessing the relative bioavailability of dust to these sites compared to within-ecosystem sources, should be major goals of future research.

CRediT authorship contribution statement

S.M. Aarons: Conceptualization, Investigation, Writing - original draft, Writing - review & editing, Visualization, Methodology. **L.J. Arvin:** Investigation, Methodology. **S.M. Aciego:** Conceptualization, Resources, Funding acquisition, Investigation, Writing - review & editing, Visualization, Methodology. **C.S. Riebe:** Conceptualization, Resources, Funding acquisition, Investigation, Writing - review & editing, Visualization, Methodology. **K.R. Johnson:** Investigation, Writing - review & editing. **M.A. Blakowski:** Investigation, Writing - review & editing. **J.M Koornneef:** Investigation, Writing - review & editing. **S.C. Hart:** Conceptualization, Resources, Funding acquisition,

Writing - review & editing. **M.E. Barnes:** Investigation, Writing - review & editing. **N. Dove:** Investigation, Writing - review & editing. **J.K. Botthoff:** Investigation. **M. Maltz:** Investigation. **E.L. Aronson:** Conceptualization, Resources, Funding acquisition, Writing - review & editing.

Declaration of Competing Interest

The authors declare that they have no known competing financial interests or personal relationships that could have appeared to influence the work reported in this paper.

Acknowledgments

This research is part of the Southern Sierra Critical Zone Observatory, which is funded by the National Science Foundation (EAR 1331939). This research is funded by the National Science Foundation under grants EAR 1744089 and 1449197, ICER 1541047, and USDA NIFA HATCH grant CA-R-PPA-5093-H. The authors of this study wish to acknowledge E. Stacy for field logistics and assistance with editing this manuscript.

Appendix A. Supplementary data

Supplementary data to this article can be found online at https://doi.org/10.1016/j.aeolia.2019.100545.

References

Aarons, S.M., Aciego, S.M., Gabrielli, P., Delmonte, B., Koornneef, J.M., Uglietti, C., Wegner, A., Blakowski, M.A., Bouman, C., 2016. Ice core record of dust sources in the western United States over the last 300 years. Chem. Geol. 442, 160–173.

Aarons, S.M., Aciego, S.M., Gleason, J.D., 2013. Variable Hf-Sr-Nd radiogenic isotopic compositions in a Saharan dust storm over the Atlantic: implications for dust flux to oceans, ice sheets and the terrestrial biosphere. Chem. Geol. 349–350, 18–26.

Aarons, S.M., Aciego, S.M., Arendt, C.A., Blakowski, M.A., Steigmeyer, A., Gabrielli, P., Sierra-Hernández, R., Beaudon, E., Delmonte, B., Baccolo, G., May, N.K.P., 2017b. Dust composition changes from Taylor Glacier (East Antarctica) during the last glacial-interglacial transition: a multi-proxy approach. Quat. Sci. Rev. 162, 60–71.

Aarons, S.M., Blakowski, M.A., Aciego, S.M., Stevenson, E.I., Sims, K.W.W., Scott, S.R., Aarons, C., 2017a. Geochemical characterization of critical dust source regions in the American West. Geochim. Cosmochim. Acta 215, 141–161.

Aciego, S.M., Bourdon, B., Lupker, M., Rickli, J., 2009. A new procedure for separating and measuring radiogenic isotopes (U, Th, Pa, Ra, Sr, Nd, Hf) in ice cores. Chem. Geol. 266, 194–204.

Aciego, S.M., Riebe, C.S., Hart, S.C., Blakowski, M.A., Carey, C.J., Aarons, S.M., Dove, N.C., Botthoff, J.K., Sims, K.W.W., Aronson, E.L., 2017. Dust outpaces bedrock in nutrient supply to montane forest ecosystems. Nat. Commun. 8.

AghaKouchak, A., Cheng, L., Mazdiyasni, O., Farahmand, A., 2014. Global warming and changes in risk of concurrent climate extremes: Insights from the 2014 California drought: global warming and concurrent extremes. Geophys. Res. Lett. 41 (24), 8847–8852. https://doi.org/10.1002/2014GL062308.

Arvin, L.J., Riebe, C.S., Aciego, S.M., Blakowski, M.A., 2017. Global patterns of dust and bedrock nutrient supply to montane ecosystems. Sci. Adv. 3, eaao1588.

Asner, G.P., Brodrick, P.G., Anderson, C.B., Vaughn, N., Knapp, D.E., Martin, R.E., 2016. Progressive forest canopy water loss during the 2012-2015 California drought. Proceedings of the National Academy of Sciences of the United States of America.

Ault, A.P., Williams, C.R., White, A.B., Neiman, P.J., Creamean, J.M., Gaston, C.J., Ralph, F.M., Prather, K.A., 2011. Detection of Asian dust in California orographic precipitation. J. Geophys. Res. Atmos. 116.

Baker, A.R., Croot, P.L., 2010. Atmospheric and marine controls on aerosol iron solubility in seawater. Mar. Chem. 120, 4–13.

Biscaye, P., Grousset, F., Revel, M., Van der Gaast, S., Zielinski, G., Vaars, A., Kukla, G., 1997. Asian provenance of glacial dust (stage 2) in the Greenland Ice Sheet project 2 ice core, Summit, Greenland. J. Geophys. Res. 102, 765–781.

Blum, J.D., Erel, Y., 1997. Rb-Sr isotope systematics of a granitic soil chronosequence: the importance of biotite weathering. Geochim. Cosmochim. Acta 61, 3193–3204.

Brahney, J., Ballantyne, A., Kociolek, P., Leavitt, P.R., Farmer, G.L., Neff, J.C., 2015. Ecological changes in two contrasting lakes associated with human activity and dust transport in western Wyoming. Limonol. Oceanogr. 60, 678–695.

Brahney, J., Ballantyne, A.P., Kociolek, P., Spaulding, S., Otu, M., Porwoll, T., Neff, J.C., 2014. Dust mediated transfer of phosphorus to alpine lake ecosystems of the Wind River Range, Wyoming, USA. Biogeochemistry 120, 259–278.

Brahney, J., Ballantyne, A.P., Sievers, C., Neff, J.C., 2013. Increasing Ca2+ deposition in the western US: the role of mineral aerosols. Aeolian Res. 10, 77–87.

California Department of Water Resources, 2018. Water year 2017: What a difference a year makes, Memorandum Report.

Cannon, F., Hecht, C.W., Cordeira, J.M., Ralph, F.M., 2018. Synoptic and mesoscale forcing of southern California extreme precipitation. J. Geophys. Res. Atmos. 123.

Chadwick, O.A., Derry, L.A., Vitousek, P.M., Huebert, B.J., Hedin, L.O., 1999. Changing sources of nutrients during four million years of ecosystem development. Nature 397, 491–497.

Chen, J., Li, G.J., Yang, J.D., Rao, W.B., Lu, H.Y., Balsam, W., Sun, Y.B., Ji, J.F., 2007. Nd and Sr isotopic characteristics of Chinese deserts: Implications for the provenances of Asian dust. Geochim. Cosmochim. Acta 71, 3904–3914.

Coble, A.A., Hart, S.C., Ketterer, M.E., Newman, G.S., Kowler, A.L., 2015. Strontium source and depth of uptake shifts with substrate age in semiarid ecosystems. J. Geophys. Res. Biogeosci. 120, 1069–1077.

Cook, B.I., Ault, T.R., Smerdon, J.E., 2015. Unprecedented 21st century drought risk in the American Southwest and Central Plains. Sci. Adv. 1.

Cook, B.I., Smerdon, J.E., Seager, R., Coats, S., 2014. Global warming and 21st century drying. Clim. Dyn. 43, 2607–2627.

Dastrup, D.B., Carling, G.T., Collins, S.A., Nelson, S.T., Fernandez, D.P., Tingey, D.G., Hahnenberger, M., Aanderud, Z.T., 2018. Aeolian dust chemistry and bacterial communities in snow are unique to airshed locations across northern Utah, USA. Atmos. Environ. 193, 251–261.

Delmonte, B., Petit, J.R., Maggi, V., 2002. Glacial to Holocene implications of the new 27000-year dust record from the EPICA Dome C (East Antarctica) ice core. Clim. Dyn. 18, 647–660.

DePaolo, D.J., 1981. A neodymium and strontium isotopic study of the Mesozoic calc-alkaline granitic batholiths of the Sierra Nevada and Peninsular Ranges, California. J. Geophys. Res. 86, 10470–10488.

Diffenbaugh, N.S., Swain, D.L., Touma, D., 2015. Anthropogenic warming has increased drought risk in California. PNAS 112, 3921–3936.

Draxler, R.R., Hess, G.D., 1998. An overview of the HYSPLIT 4 modelling system for trajectories, dispersion, and deposition. Aust. Meteorol. Mag. 47, 295–308.

Duce, R.A., Unni, C.K., Ray, B.J., Prospero, J.M., Merrill, J.T., 1980. Long-range atmospheric transport of soil dust from Asia to the tropical north pacific: temporal variability. Science 209 (4464), 1522–1524. https://doi.org/10.1126/science:209.4464.1522.

Evan, A.T., Fiedler, S., Zhao, C., Menut, L., Schepanski, K., Flamant, C., Doherty, O., 2015. Derivation of an observation-based map of North African dust emission. Aeolian Res. 15, 153–162.

Evan, A.T., Flamant, C., Fiedler, S., Doherty, O., 2014. An analysis of aeolian dust in climate models. Geophys. Res. Lett. 41, 5996–6001.

Evan, A.T., Flamant, C., Gaetani, M., Guichard, F., 2016. The past, present and future of African dust. Nature 531, 493–495.

Flint, L.E., Flint, A.L., Mendoza, J., Kalansky, J., Ralph, F.M., 2018. Characterizing drought in California: new drought indices and scenario-testing in support of resource management. Ecol. Process 7 (1). https://doi.org/10.1186/s13717-017-0112-6.

Frank, M., 2002. Radiogenic isotopes: tracers of past ocean circulation and erosional input. Rev. Geophys. 40 (1). https://doi.org/10.1029/2000RG000094.

Ginoux, P., Prospero, J.M., Gill, T.E., Hsu, N.C., Zhao, M., 2012. Global-scale attribution of anthropogenic and natural dust sources and their emission rates based on MODIS Deep Blue aerosol products. Rev. Geophys. 50.

Ginoux, P., Prospero, J.M., Torres, O., Chin, M., 2004. Long-term simulation of global dust distribution with the GOCART model: correlation with North Atlantic Oscillation. Environ. Modell. Software 19, 113–128.

Goldstein, S.L., O'Nions, R.K., Hamilton, P.J., 1984. A Sm-Nd isotopic study of atmospheric dusts and particulates from major river systems. Earth Planet. Sci. Lett. 70, 221–236.

Griffin, D., Anchukaitis, K.J., 2014. How unusual is the 2012–2014 California drought? Geophys. Res. Lett. 41, 9017–9023.

Grousset, F.E., Biscaye, P.E., 2005. Tracing dust sources and transport patterns using Sr, Nd and Pb isotopes. Chem. Geol. 222, 149–167.

Grousset, F.E., Biscaye, P.E., Revel, M., Petit, J.-R., Pye, K., Joussaume, S., Jouzel, J., 1992. Antarctic (Dome C) ice-core dust at 18 k.y. B.P.: Isotopic constraints on origins. Earth Planet. Sci. Lett. 111, 175–182.

Guo, H., Bao, A., Liu, T., Jiapaer, G., Ndayisaba, F., Jiang, L., Kurban, A., De Maeyer, P., 2018. Spatial and temporal characteristics of droughts in Central Asia during 1966–2015. Sci. Total Environ. 624, 1523–1538.

Hawkings, J.R., Benning, L.G., Raiswell, R., Kaulich, B., Araki, T., Abyaneh, M., Stockdale, A., Koch-Muller, M., Wadham, J.L., Tranter, M., 2018. Biolabile ferrous iron bearing nanoparticles in glacial sediments. Earth Planet. Sci. Lett. 493, 92–101.

Hessl, A.E., Anchukaitis, K.J., Jelsema, C., Cook, B., Byambasuren, O., Leland, C., Nachin, B., Pederson, N., Tian, H., Hayles, L.A., 2018. Past and future drought in Mongolia. Sci. Adv. 4, e1701832.

Howitt, R.E., MacEwan, D., Medellín-Azuara, J., Lund, J.R., Sumner, D.A., 2015. Economic Analysis of the 2015 Drought for California Agriculture. Center for Watershed Sciences, University of California-Davis, Davis, CA, pp. 16.

Husar, R.B., Tratt, D.M., Schichtel, B.A., Falke, S.R., Li, F., Jaffe, D., Gassó, S., Gill, T., Laulainen, N.S., Lu, F., Reheis, M.C., Chun, Y., Westphal, D., Holben, B.N., Gueymard, C., McKendry, I., Kuring, N., Feldman, G.C., McClain, C., Frouin, R.J., Merrill, J., DuBois, D., Vignola, F., Murayama, T., Nickovic, S., Wilson, W.E., Sassen, K., Sugimoto, N., Malm, W.C., 2001. Asian dust events of April 1998. J. Geophys. Res. Atmos. 106, 18317–18330.

Ingram, B.L., Lin, J.C., 2002. Geochemical tracers of sediment sources to San Francisco Bay. Geology 30, 575–578.

Jacobsen, S.B., Wasserberg, G.J., 1980. Sm-Nd isotopic evolution of chondrites. Earth Planet. Sci. Lett. 50, 139–155.

Jiao, L., Wang, X., Li, D., 2018. Spatial variation in the flux of atmospheric deposition and its ecological effects in arid Asia. Aeolian Res. 32, 71–91.

Jickells, T.D., An, Z.S., Andersen, K.K., Baker, A.R., Bergametti, G., Brooks, N., Cao, J.J.,

Boyd, P.W., Duce, R.A., Hunter, K.A., Kawahata, H., Kubilay, N., laRoche, J., Liss, P.S., Mahowald, N., Prospero, J.M., Ridgwell, A.J., Tegen, I., Torres, R., 2005. Global iron connections between desert dust, ocean biogeochemistry, and climate. Science 308, 67–71.
Jweda, J., Bolge, L., Class, C., Goldstein, S.L., 2015. High precision Sr-Nd-Hf-Pb isotopic compositions of USGS reference material BCR-2. Geostand. Geoanal. Res.
Kanayama, S., Yabuki, S., Yanagisawa, F., Motoyama, R., 2002. The chemical and strontium isotope composition of atmospheric aerosols over Japan: the contribution of long-range-transported Asian dust (Kosa). Atmos. Environ. 36, 5159–5175.
Kanayama, S., Yabuki, S., Zeng, F.J., Liu, M.Z., Shen, Z.B., Liu, L.C., Yanagisawa, F., Abe, O., 2005. Size-dependent geochemical characteristics of Asian dust - Sr and Nd isotope compositions as tracers for source identification. J. Meteorol. Soc. Jpn 83A, 107–120.
Kim, H., Choi, M., 2015. Impact of soil moisture on dust outbreaks in East Asia: using satellite and assimilation data. Geophys. Res. Lett. 42, 2789–2796.
Kohfeld, K., Harrison, S., 2001. DIRTMAP: the geological record of dust. Earth Sci. Rev. 54, 81–114.
Koornneef, J.M., Bouman, C., Schwieters, J.B., Davies, G.R., 2014. Measurement of small ion beams by thermal ionisation mass spectrometry using new 10^{13} Ohm resistors. Anal. Chim. Acta 819, 49–55.
Koornneef, J.M., Nikogosian, I., van Bergen, M.J., Smeets, R., Bouman, C., Davies, G.R., 2015. TIMS analysis of Sr and Nd isotopes in melt inclusions from Italian potassium-rich lavas using prototype 10^{13} Ω amplifiers. Chem. Geol. 397, 14–23.
Kurtz, A.C., Derry, L.A., Chadwick, O.A., 2001. Accretion of Asian dust to Hawaiian soils: isotopic, elemental, and mineral mass balances. Geochim. Cosmochim. Acta 65, 1971–1983.
Li, X., Waddington, S.R., Dixon, J., Joshi, A.K., Vicente, M.C., 2011. The relative importance of drought and other water-related constraints for major food crops in South Asian farming systems. Food Security 3, 19–33.
Lybrand, R.A., Rasmussen, C., 2017. Climate, topography, and dust influences on the mineral and geochemical evolution of granitic soils in southern Arizona. Geoderma 314, 245–261.
Mahowald, N., 2011. Aerosol indirect effect on biogeochemical cycles and climate. Science 334, 794–796.
Mahowald, N., Kloster, S., Engelstaedtler, S., Moore, J.K., Mukhopadhyay, S., McConnell, J.R., Albani, S., Doney, S.C., Bhattacharya, A., Curran, M.A.J., Flanner, M.G., Hoffman, F.M., Lawrence, D.M., Lindsay, K., Mayewski, P.A., Neff, J., Rothenberg, D., Thomas, E.P.E.T., Zender, C.S., 2010. Observed 20th century desert dust variability: impact on climate and biogeochemistry. Atmos. Chem. Phys. 10, 10875–10893.
Mahowald, N.M., Muhs, D.R., Levis, S., Rasch, P.J., Yoshioka, M., Zender, C.S., Luo, C., 2006. Change in atmospheric mineral aerosols in response to climate: last glacial period, preindustrial, modern, and doubled carbon dioxide climates. J. Geophys. Res. Atmos. 111.
Martin, J.A.R., Arana, C.D., Miras, J.J.R., Gil, C., Boluda, R., 2015. Impact of 70 years urban growth associated with heavy metal pollution. Environ. Pollut. 196, 156–163.
Martin, J.H., 1990. Glacial-interglacial CO2 change: the iron hypothesis. Paleoceanography 5, 1–13.
Martínez-Garcia, A., Rosell-Melé, A., Jaccard, S.L., Geibert, W., Sigman, D.M., Haug, G.H., 2011. Southern ocean dust-climate coupling over the past four million years. Nature 476, 312–315.
Martínez-Garcia, A., Sigman, D.M., Ren, H., Anderson, R.F., Straub, M., Hodell, D.A., Jaccard, S.L., Eglinton, T.I., Haug, G.H., 2014. Iron fertilization of the subantarctic ocean during the last ice age. Science 343, 1347–1350.
Munkhtsetseg, E., Shinoda, M., Gillies, J.A., Kimura, R., King, J., Nikolich, G., 2016. Relationships between soil moisture and dust emissions in a bare sandy soil of Mongolia. Particuology 28, 131–137.
Neff, J.C., Ballantyne, A.P., Farmer, G.L., Mahowald, N.M., Conroy, J.L., Landry, C.C., Overpeck, J.T., Painter, T.H., Lawrence, C.R., Reynolds, R.L., 2008. Increasing eolian dust deposition in the western United States linked to human activity. Nat. Geosci. 1, 189–195.
Nriagu, J.O., Pacyna, J.M., 1988. Quantitative assessment of worldwide contamination of air, water and soils by trace metals. Nature 333, 134–139.
O'Nions, R.K., Carter, S.R., Evensen, N.M., Hamilton, P.J., 1979. Geochemical and cosmochemical applications of Nd isotope analysis. Ann. Rev. Earth Planet. Sci. Lett. 7, 11–38.
Pett-Ridge, J.C., Derry, L.A., Kurtz, A.C., 2009. Sr isotopes as a tracer of weathering processes and dust inputs in a tropical granitoid watershed, Luquillo Mountains, Puerto Rico. Geochim. Cosmochim. Acta 73, 25–43.
Ponette-Gonzalez, A.G., Collins, J.D., Manuel, J.E., Byers, T.A., Glass, G.A., Weathers, K.C., Gill, T.E., 2018. Wet dust depositions across Texas during the 2012 drought: an overlooked pathways for elemental flux to ecosystems. J. Geophys. Res. Atmos. 123, 8238–8254.
Porder, S., Hilley, G.E., Chadwick, O.A., 2007. Chemical weathering, mass loss, and dust inputs across a climate by time matrix in the Hawaiian Islands. Earth Planet. Sci. Lett. 258, 414–427.
Pourmand, A., Prospero, J.M., Sharifi, A., 2014. Geochemical fingerprinting of trans-Atlantic African dust based on radiogenic Sr-Nd-Hf isotopes and rare earth element anomalies. Geology 42, 675–678.
Prospero, J.M., Ginoux, P., Torres, O., Nicholson, S.E., Gill, T.E., 2002. Environmental characterization of global sources of atmospheric soil dust identified with the Nimbus 7 Total Ozone Mapping Spectrometer (TOMS) absorbing aerosol product. Rev. Geophys. 40.
Prospero, J.M., Lamb, P.J., 2003. African droughts and dust transport to the Caribbean: climate change implications. Science 302, 1024–1027.
Prospero, J.M., Nees, R.T., 1986. Impact of the North African drought and El Nino on mineral dust in the Barbados trade winds. Nature 320, 735–738.
Reheis, M.C., Budahn, J.R., Lamothe, P.J., 2002. Geochemical evidence for diversity of dust sources in the southwestern United States. Geochim. Cosmochim. Acta 66, 1569–1587.
Reynolds, R.L., Reheis, M., Yount, J., Lamothe, P., 2006b. Composition of aeolian dust in natural traps on isolated surfaces of the central Mojave Desert-Insights to mixing, sources, and nutrient inputs. J. Arid Environ. 66, 42–61.
Rosenbauer, R.J., Foxgrover, A.C., Hein, J.R., Swarzenski, P.W., 2013. A Sr-Nd isotopic study of sand-sized sediment provenance and transport for the San Francisco Bay coastal system. Mar. Geol. 345, 143–153.
Rotberg, G.L., 2008. New Geochemical and Geochronogic Data from the Northern Sierra Nevada, California: Constraints on the Preconditions for Lithospheric Foundering. Department of Geosciences, University of Arizona, Tucson, Arizona.
Scheuvens, D., Schütz, L., Kandler, K., Ebert, M., Weinbruch, S., 2013. Bulk composition of northern African dust and its source sediments-a compilation. Earth Sci. Rev. 116, 170–194.
Schroth, A.W., Crusius, J., Sholkovitz, E.R., Bostick, B.C., 2009. Iron solubility driven by speciation in dust sources to the ocean. Nat. Geosci. 2, 337–340.
Shao, Y.P., Klose, M., Wyrwoll, K.H., 2013. Recent global dust trend and connections to climate forcing. J. Geophys. Res. Atmos. 118, 11107–11118.
Shoenfelt, E.M., Sun, J., Winckler, G., Kaplan, M.R., Borunda, A.L., Farrell, K.R., Moreno, P.I., Gaiero, D.M., Recasens, C., Sambrotto, R.N., Bostick, B.C., 2017. High particulate iron(II) content in glacially sourced dusts enhances productivity of a model diatom. Sci. Adv. 3 (6), e1700314. https://doi.org/10.1126/sciadv.1700314.
Spokes, J.L., Jickells, T.D., Lim, B., 1994. Solubilisation of aerosol trace metals by cloud processing: a laboratory study. Geochim. Cosmochim. Acta 58, 3281–3287.
Stephens, S.L., Collins, B.M., Fettig, C.J., Finney, M.A., Hoffman, C.M., Knapp, E.E., North, M.P., Safford, H., Wayman, R.B., 2018. Drought, tree mortality, and wildfire in forests adapted to frequent fire. Bioscience 68 (2), 77–88.
Stewart, B.W., Capo, R.C., Chadwick, O.A., 2001. Effects of rainfall on weathering rate, base cation provenance, and Sr isotope composition of Hawaiian soils. Geochim. Cosmochim. Acta 65, 1087–1099.
Stockdale, A., Krom, M.D., Mortimer, R.J.G., Benning, L.G., Carslaw, K.S., Herbert, R.J., Shi, Z., Myriokefalitakis, S., Kanakidou, M., Nenes, A., 2016. Understanding the nature of atmospheric acid processing of mineral dusts in supplying bioavailable phosphorus to the oceans. PNAS 113, 14639–14644.
Stohl, A., 1998. Computation, accuracy and applications of trajectories-a review and bibliography. Atmos. Environ. 32, 947–966.
Suvarapu, L.N., Baek, S.-O., 2017. Determination of heavy metals in the ambient atmosphere: a review. Toxicol. Ind. Health 33, 79–96.
Swain, D.L., Tsiang, M., Haugen, M., Singh, D., Charland, A., Rajaratnam, B., Diffenbaugh, N.S., 2014. The extraordinary California drought of 2013–2014: character, context, and the role of climate change. Bull. Am. Meterol. Soc. 95, S3–S7.
Uddin, M.K., 2017. A review on the adsorption of heavy metals by clay minerals, with special focus on the past. Chem. Eng. J. 308, 438–462.
US National Climate Data Center, 2014. National Climate Data Center NNDC Climate Data Online. Available at. www7.ncdc.noaa.gov/CDODivisionalSelect.jsp.
van der Does, M., Pourmand, A., Sharifi, A., Stuut, J.-B.W., 2018. North African mineral dust across the tropical Atlantic Ocean: Insights from dust particle size, radiogenic Sr-Nd-Hf isotopes and rare earth elements (REE). Aeolian Res. 33, 106–116.
van Mantgem, P.J., Nesmith, J.C.B., Keifer, M.M., Knapp, E.E., Flint, A.L., Flint, L.E., 2013. Climatic stress increases forest fire severity across the western United States. Ecol. Lett. 16, 1151–1156.
Vicars, W.C., Sickman, J.O., 2011. Mineral dust transport to the Sierra Nevada, California: loading rates and potential source areas. J. Geophys. Res. Biogeosci. 116.
Vicente-Serrano, S.M., Begueria, S., Lopez-Moreno, J.I., 2010. A Multi-scalar drought index sensitive to global warming: The Standardized Precipitation Evapotranspiration Index-SPEI. J. Clim. 23, 1696–1718.
Wang, H., He, S., 2015. The north China/northeastern Asia severe summer drought in 2014. J. Climate 28 (17), 6667–6681. https://doi.org/10.1175/JCLI-D-15-0202.1.
Wedepohl, K.H., 1995. The composition of the continental crust. Geochim. Cosmochim. Acta 59, 1217–1232.
White, W.M., 2013. Geochemistry. Wiley-Blackwell.
Wilkening, K.E., Barrie, L.A., Engle, M., 2000. Trans-pacific air pollution. Science 290, 65–67.
Yokoo, Y., Nakano, T., Nishikawa, M., Quan, H., 2004. Mineralogical variation of Sr-Nd isotopic and elemental compositions in loess and desert sand from the central Loess Plateau in China as a provenance tracer of wet and dry deposition in the northwestern Pacific. Chem. Geol. 204, 45–62.
Zhang, L., Zhou, T., 2015. Drought over East Asia: a review. J. Clim. 28 (8), 3375–3399. https://doi.org/10.1175/JCLI-D-14-00259.1.